

# Passively Q-switched erbium-doped fiber laser using evanescent field interaction with gold-nanosphere based saturable absorber

Dengfeng Fan,<sup>1</sup> Chengbo Mou,<sup>2,3</sup> Xuekun Bai,<sup>1</sup> Shaofei Wang,<sup>1</sup>  
Na Chen,<sup>1</sup> and Xianglong Zeng<sup>1,\*</sup>

<sup>1</sup>The Key Lab of Specialty Fiber Optics and Optical Access Network, Shanghai University,  
200072 Shanghai, China

<sup>2</sup>Aston Institute of Photonic Technologies (AIPT), School of Engineering and Applied Science,  
Aston University, Birmingham, B4 7ET, UK

<sup>3</sup>mouc1@aston.ac.uk

\*zenglong@shu.edu.cn

**Abstract:** We demonstrate an all-fiber passively Q-switched erbium-doped fiber laser (EDFL) using a gold-nanosphere (GNS) based saturable absorber (SA) with evanescent field interaction. Using the interaction of evanescent field for fabricating SAs, long nonlinear interaction length of evanescent wave and GNSs can be achieved. The GNSs are synthesized from mixing solution of chloroauric acid ( $\text{HAuCl}_4$ ) and sodium citrate by the heating effects of the microfiber's evanescent field radiation. The proposed passively Q-switched EDFL could give output pulses at 1562 nm with pulse width of 1.78  $\mu\text{s}$ , a repetition rate of 58.1 kHz, a pulse energy of 133 nJ and a output power of 7.7 mW when pumped by a 980 nm laser diode of 237 mW.

© 2014 Optical Society of America

**OCIS codes:** (140.3510) Lasers, fiber; (140.3540) Lasers, Q-switched; (160.4330) Nonlinear optical materials.

---

## References and links

1. F. Kong, L. Liu, C. Sanders, Y. C. Chen, and K. K. Lee, "Phase locking of nanosecond pulses in a passively Q-switched two-element fiber laser array," *Appl. Phys. Lett.* **90**, 151110 (2007).
2. P. Pérez-Millán, J. L. Cruz, and M. V. Andrés, "Active Q-switched distributed feedback erbium-doped fiber lasers," *Appl. Phys. Lett.* **87**, 011104 (2005).
3. J. Liu, W. Sida, Q. Yang, and P. Wang, "Stable nanosecond pulse generation from a graphene-based passively Q-switched Yb-doped fiber laser," *Opt. Lett.* **36**(20), 4008–4010 (2011).
4. D. Zhou, L. Wei, B. Dong, and W. Liu, "Tunable passively Q-switched erbium-doped fiber laser with carbon nanotubes as a saturable absorber," *IEEE Photon. Technol. Lett.* **22**(1), 9–11 (2010).
5. L. Pan, I. Utkin, and R. Fedosejevs, "Passively Q-switched ytterbium-doped double-clad fiber laser with a  $\text{Cr}^{4+}$ : YAG saturable absorber," *IEEE Photon. Technol. Lett.* **19**(24), 1979–1981 (2007).
6. J. Xu, X. Li, Y. Wu, X. Hao, J. He, and K. Yang, "Graphene saturable absorber mirror for ultra-fast-pulse solid-state laser," *Opt. Lett.* **36**(10), 1948–1950 (2011).
7. B. Dong, J. Hu, C. Liaw, J. Hao, and C. Yu, "Wideband-tunable nanotube Q-switched low threshold erbium doped fiber laser," *Appl. Opt.* **50**(10), 1442–1445 (2011).
8. M. Amos, K. Fuse, B. Xu, and S. Yamashita, "Optical deposition of graphene and carbon nanotubes in a fiber ferrule for passive mode-locked lasing," *Opt. Express* **18**(22), 23054–23061 (2010).
9. H. Liu, K. Chow, S. Yamashita, and S. Set, "Carbon-nanotube-based passively Q-switched fiber laser for high energy pulse generation," *Opt. Laser Technol.* **45**, 713–716 (2013).
10. H. Liao, R. Xiao, J. Fu, P. Yu, G. Wong, and P. Sheng, "Large third-order optical nonlinearity in Au:  $\text{SiO}_2$  composite films near the percolation threshold," *Appl. Phys. Lett.* **70**, 1–3 (1997).

11. M. B. Mohamed and M. A. El-Sayed, "Femtosecond excitation dynamics in gold nanospheres and nanorods," *Phys. Rev. B* **72**, 235405 (2005).
12. X. Huang, W. Qian, I. H. El-Sayed, and M. A. El-sayed, "The potential use of the enhanced nonlinear properties of gold nanospheres in photothermal cancer therapy," *Lasers Med. Sci.* **39**, 747–753 (2007).
13. K. Tsuboi, S. Fukuba, M. Shimojo, M. Tanaka, K. Furuya, K. Fujita, and K. Kajikawa, "Second-harmonic spectroscopy of surface immobilized gold nanospheres above a gold surface supported by self-assembled monolayers," *J. Chem. Phys.* **125**, 174703 (2006).
14. T. Jiang, Y. Xu, Q. Tian, L. Liu, Z. Kang, R. Yang, G. Qin, and W. Qin, "Passively Q-switching induced by gold nanocrystals," *Appl. Phys. Lett.* **101**, 151122 (2012).
15. Z. Kang, X. Guo, Z. Jia, Y. Xu, L. Liu, D. Zhao, G. Qin, and W. Qin, "Gold nanorods as saturable absorbers for all-fiber passively Q-switched erbium-doped fiber laser," *Opt. Mater. Express* **3**(11), 1986–1991 (2013).
16. T. Jiang, Z. Kang, G. Qin, J. Zhou, and W. Qin, "Low mode-locking threshold induced by surface plasmon field enhancement of gold nanoparticles," *Opt. Express* **21**(23), 27992–28000 (2013).
17. Z. Kang, Y. Xu, L. Zhang, Z. Jia, L. Liu, D. Zhao, Y. Feng, G. Qin, and W. Qin, "Passively mode-locking induced by gold nanorods in erbium-doped fiber lasers," *Appl. Phys. Lett.* **103**, 041105 (2013).
18. T. A. Birks and Y. W. Li, "The shape of fiber tapers," *J. Lightwave Technol.* **10**(4), 432–438 (1992).
19. Q. Fan, J. Cao, Y. Liu, B. Yao, and Q. Mao, "Investigations of the fabrication and the surface enhanced applications for tapered fiber probes prepared with the laser-induced chemical deposition method," *Appl. Opt.* **52**(25), 6163–6169 (2013).
20. J. Wang, Z. Luo, M. Zhou, C. Ye, H. Fu, Z. Cai, H. Cheng, H. Xu, and W. Qi, "Evanescent-light deposition of graphene onto tapered fibers for passive Q-switch and mode-locker," *IEEE Photon. J.* **4**(5), 1295–1305 (2012).
21. Y. Cui, P. P. Shum, G. Wang, H. Chang, X. Q. Dinh, M. Jiang, and G. Humbert, "Size effect of gold nanoparticles on optical microfiber refractive index sensors," in *Proceedings of Sensor*, Limerick, Ireland (IEEE, 2011), pp. 371–374.
22. W. Shin and K. Oh, "Analysis and Measurement of the OH absorption induced loss in a tapered single mode optical fiber," in *Proceedings of Conference of Lasers and Electro-Optics* (IEEE, 2002), pp. 237–238.
23. B. Dong, J. Hao, J. Hu, and C. Liaw, "Wide pulse-repetition-rate range tunable nanotube-switched low threshold erbium-doped fiber laser," *IEEE Photon. Technol. Lett.* **22**(24), 1853–1855 (2010).
24. G. Sobon, J. Sotor, J. Jagiello, R. Kozinski, K. Librant, M. Zdrojek, L. Lipinska and K. M. Abramski, "Linearly polarized, Q-switched Er-doped fiber laser based on reduced graphene oxide saturable absorber," *Appl. Phys. Lett.* **101**, 241106 (2012).
25. Z. C. Tiu, F. Ahmad, S. J. Tan, H. Ahmad, and S. W. Harun, "Passive Q-switched Erbium-doped fiber laser with graphene-polyethylene oxide saturable absorber in three different gain media," *Indian J Phys.* **88**(7), 727–731 (2014).
26. J. Y. Huang, S. C. Huang, H. L. Chang, K. W. Su, Y. F. Chen, and K. F. Huang, "Passive Q switching of Er-Yb fiber laser with semiconductor saturable absorber," *Opt. Express* **16**(5), 3002–3007 (2008).

## 1. Introduction

Q-switched fiber lasers have been paid much attention owing to their extensive applications for telecommunications, medicine, military, material processing, optical fiber sensing etc [1–4]. They provide relatively large pulse energy at relatively low repetition rates and pulse width of the scale from microsecond to nanosecond compared to the mode locked fiber lasers that generate relatively short but low single energy pulses. Q-switched pulses can be obtained via active or passive Q-switching techniques. Passively Q-switched erbium-doped fiber lasers (EDFLs) have advantages on the aspects of compactness, simplicity and low cost in design compared to those using the active technique such as electro-optic and acousto-optic modulators. They have been widely investigated by utilizing different kinds of saturable absorbers (SAs) such as transition metal doped crystals [5] and semiconductor SAs like graphene [6]. Currently, nanomaterials such as graphene and carbon nanotubes (CNTs) are considered to be the ideal SAs for realizing all-fiber Q-switched fiber lasers due to their advantages such as wide absorption wavelength bandwidth, ultrafast recovery time and simple manufacturing process [6–9]. All-fiber passively Q-switched EDFLs with CNTs or graphene SAs have been demonstrated [4, 9]. Recently, much work has been carried out on the synthesis of CNTs and graphene with different layers to maintain better performance of Q-switching such as pulse energy [9].

Gold-nanosphere (GNS) has a large third-order nonlinearity and ultrafast response time about few picoseconds which have the application in ultrafast optics, medical science and spectroscopy

[10–13]. Picoseconds recovery time of GNS-based SAs promises for getting Q-switched pulses. Recently, Tao Jiang *et al* reported that they made SAs of gold nanoparticles and gold nanorods film for Q-switched pulses and mode locked pulses by sandwiching them between two fiber connectors [14–17]. Although this fiber ferrule connection method offers easy implementation of the SA, it breaks the all-fiber configuration of the laser cavity. Furthermore, the mechanical contact induced physical damage of the SA could not be well controlled when using this approach. This method also suffers from physical damage under high power regimes especially in the case of polymer composite. Using the evanescent field interaction based SA, both high modulation depth and high damage threshold can be obtained owing to a controllable nonlinear interaction length. Additionally, the Q-switched fiber laser based on evanescent field interaction SA could maintain the all-fiber format.

In this work, we propose and demonstrate an all-fiber passively Q-switched EDFL by using the interaction of GNSs and the microfiber's evanescent fields, which achieves output pulses at 1562 nm with a pulse width of 1.78  $\mu$ s, a repetition rate of 58.1 kHz, a single pulse energy of 133 nJ and an output power of 7.7 mW pumped via a 980 nm laser diode for a pump power of  $\sim$ 237 mW.

## 2. Fabrication and characterization of GNS-based SA

The GNS-based SA for Q-switched EDFL in this paper is made by depositing GNSs on a microfiber, which is fabricated by using the standard flame brushing technique [18]. Generally, the waist diameter and the length of the microfiber we used here could be fabricated down to about 5  $\mu$ m and 2 cm with the insertion loss of about 0.2 dB.

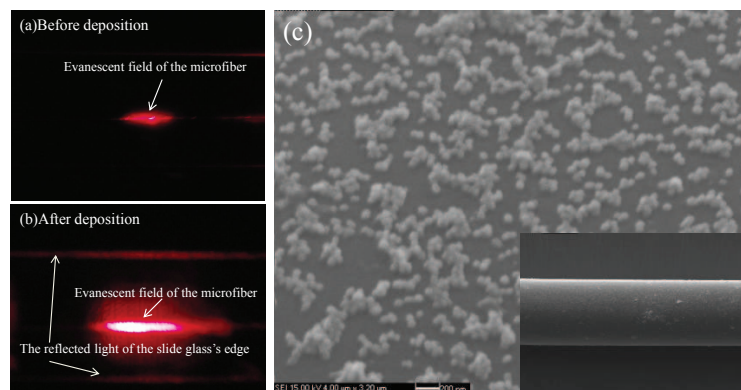


Fig. 1. The same microfiber under different states. (a) The evanescent field of the microfiber by injecting a red light. (b) The stronger evanescent field radiation of the injecting red light after depositing GNSs. (c) SEM image of the GNSs deposited on the surface of the microfiber. The insertion is the microfiber deposited with GNSs.

The microfiber is then glued on a glass slide. Strong evanescent field radiation of the injecting red light was observed as shown in Fig. 1(a). The GNSs prepared here are synthesized by mixing the solution of  $\text{HAuCl}_4$  and sodium citrate. 1 ml 1wt.%  $\text{HAuCl}_4$  solution is added to 10 ml ultrapure water for dilution in the prepared cleaning beaker. At the same time, 0.5 ml 1wt.% sodium citrate solution diluted by 1 ml ultrapure water is added to  $\text{HAuCl}_4$  solution. The mixed solutions are stirred softly and slowly for few seconds, and then dripped onto the microfiber by a transfer liquid gun. To deposit GNSs on the microfiber, a laser light (532 nm) with 100 mW input power is injected into the microfiber for 20 min in our experiments. The GNSs are deposited by heating effect induced through the evanescent field radiation [19] and therefore easy

to be attached to the microfiber's surface by the heat convection effects. Figure 1(b) shows the stronger evanescent field radiation of the injecting red light after depositing GNSs than that before deposition due to the scattering of GNSs on the surface of the microfiber exhibiting similar behavior to a graphene based device [20]. Figure 1(c) shows the SEM image of GNSs deposited on the microfiber while the inset shows the GNS-deposited microfiber. The diameter of GNSs distributes from 30 nm to 80 nm, which could induce surface plasmon resonance through the evanescent field interaction [21]. The inhomogeneous distribution of GNSs on the surface of the microfiber is due to the non-uniform intensity pattern from the evanescent field radiation. Finally, the fabricated GNS-based SA is exposed at room temperature to allow the evaporation of the residual solution. The measured optical transmissions of the microfiber before and after the deposition of GNSs are illustrated in Fig. 2(a). We can see that before the deposition, the microfiber has low loss across the infrared band from 1300 nm to 1700 nm. The pronounced absorption feature at 1390 nm is due to the OH in the microfiber induced from oxyhydrogen flame [22]. While after the GNSs deposition, an obvious loss induced by the evanescent field interaction has been observed. The induced broad absorption region around 1450 nm is owing to the metal surface plasmon resonance absorption resulted from surface plasma wave of gold nanospheres and the evanescent wave [14]. The saturable absorption of the SA is  $\sim 40\%$ . The measured modulation depth and the nonlinear loss of the SA is about 7.8% and 52.7% as shown in Fig. 2(b) using a home-made 1561 nm mode locked EDFL.

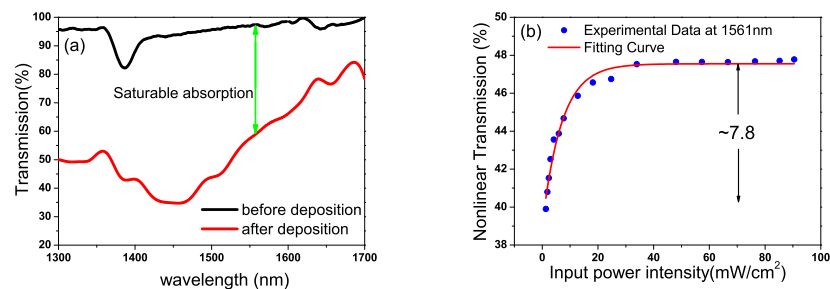


Fig. 2. (a) The transmissions of the microfiber before and after deposition of GNSs. (b) The modulation depth of the GNS-based SA.

### 3. Experiment on GNS-based passively Q-switched EDFL

Figure 3 shows the schematic configuration of the passively Q-switched EDFL combined with the fabricated GNS-based SA. A length of 7.5 m EDF is pumped by a 980 nm laser diode through a 980/1550 nm wavelength division multiplexing (WDM) coupler. The EDF used in this experiment has a nominal absorption of  $6.0 \pm 1.0$  dB/m at 1530 nm (NUFERN, EDFC-980-HP) with a dispersion of  $+15.5$  ps<sup>2</sup>/km at 1550 nm. The pigtail fiber length of the WDM coupler is  $\sim 1.86$  m with a dispersion of  $-0.25$  ps<sup>2</sup>/km at 1550 nm (Corning, HICER98 specialty optical fibers). A polarization-independent isolator (PI-ISO) is utilized to force the unidirectional operation of the laser cavity. 10% of the output power is extracted from the laser cavity as the laser output by a 90/10 coupler. The rest of the fibers in the laser ring cavity are single-mode fibers (SMFs) with a dispersion of  $-23$  ps<sup>2</sup>/km at 1550 nm and the total length of the cavity is about 19.4 m. The total dispersion of the cavity is about  $-0.1$  ps<sup>2</sup> at 1550 nm. Temporal and spectral profiles of the Q-switched fiber laser output are recorded by a 10 GHz electro-photon detector (CONQUER, KG-PD-10G-FP) followed by a 300 MHz oscilloscope (Tektronix, DPO3032) and an optical spectrum analyzer (YOKOGAWA, AQ6370C).

Passively Q-switching of the constructed fiber laser self-starts at an input pump power of

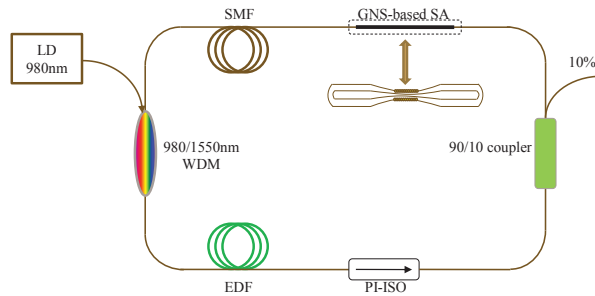


Fig. 3. The schematic of the passively Q-switched EDFL with the GNS-based SA.

114.8 mW. Such a relatively high threshold power results from the high intra-cavity loss induced by the GNS-based SA. The 3-dB bandwidth of the optical spectrum is measured to be 1.69 nm at the center wavelength of 1561.8 nm when pumping at 114.8 mW as shown in Fig. 4(a). The measured average output power is  $\sim 2.1$  mW using a commercial power meter (Yiai, AV6334). Figure 4(a) depicts its corresponding output pulse train with a repetition rate of 42.7 kHz when passively Q-switching starts. Figure 4(c) shows the measured pulse width of the Q-switched pulse is 2.7  $\mu$ s. To confirm the functionality of GNS-based SA, we insert the microfiber without GNSs deposition into the same laser cavity while no pulse generation was observed. It confirms that the Q-switched pulse generation originates from the GNS-based SA in the cavity not the bare microfiber itself. The GNS-based SA in the laser cavity functions as a loss modulator. This loss consists of both linear loss and nonlinear loss. The former is induced by the microfiber itself and the latter is due to the absorption of the SA. For conventional ring cavity fiber lasers that operate in Q-switching and prohibit from broadband mode-locking, the cavity configurations need SAs as well as narrowband filters such as fiber Bragg grating to restrain multimode oscillation, which could sacrifice the intra-cavity energy [4, 7]. In this experiment, passively Q-switching is attributed to general modulation depth of the GNSs via evanescent field interaction along a confined distance. The peak power of the intra-cavity pulse cannot rise up where fiber nonlinearity becomes important within one cavity round-trip time, therefore the laser spectrum is insufficient for broadband mode-locking and pulses are only released when the population inversion of gain medium is at its highest level [9].

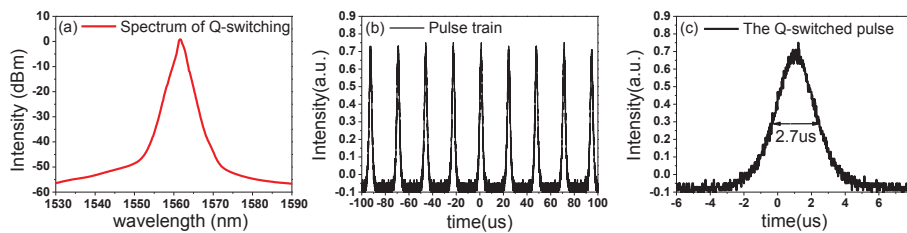


Fig. 4. (a) The spectrum of the Q-switched pulses with the 3dB bandwidth of 1.69 nm. (b) The pulse train with the repetition rate of 42.7 kHz. (c) The profile of the Q-switched pulse.

By increasing the pump power from 114.8 mW to 264.7 mW, the pulse duration of output stable pulses trains varies from 2.7  $\mu$ s to 1.7  $\mu$ s while the repetition rate monotonically increases from 42.7 kHz to 64.9 kHz as plotted in Fig. 5(a). Unlike passively mode-locking condition where the repetition rate of the output pulses is fixed corresponding to the cavity length [15, 16], the repetition rate of the proposed Q-switched EDFL can be varied with reference to the lifetime

of gain medium as well as pump power. The rather long pulse duration is mainly due to the long laser cavity length which leads to a long cavity lifetime. Since different pump powers induce different time required to replenish the extracted energy between two consecutive pulses, the detuning of repetition rate takes place. In the experiment, when more gain is provided to saturate the SA, pulse energy is found to change with the increment of the pump power and the output power increasing monotonously as shown in Fig. 5(b). The output efficiency of the laser is about 3.5%. Benefiting from the scheme of GNS-evanescent field interaction, output pulse with pulse energy of 133 nJ is achieved at the maximum pump power of 264.7 mW. The obtained pulse energy in the experiment as well as other reports using gold nanoparticles as a SA for Q-switching is found to be relatively higher than previous reports using CNT-based SAs [4, 9, 23] and graphene-based SAs [24, 25] in ring cavity. No stable pulse trains were observed when the pump power is higher than 264.7 mW. So far, there are only few reports on the GNS-SA based pulse laser except the fiber connector based GNS SA [14–17]. Also, for a Q-switched fiber laser with high pulse energy output, a lower repetition rate and higher pump power is preferred because the intra-cavity power can be more effectively coupled to each pulse. Although such pulse energy still cannot outperform the laser using conventional semiconductor-based SAs [26], further improvement for scaling up pulse energy is foreseeable with such type of SA by optimizing the design of the microfiber and synthesis of GNSs. Using other kinds of couplers such as 30/70 coupler and high gain active fiber in the cavity could also boost the output power.

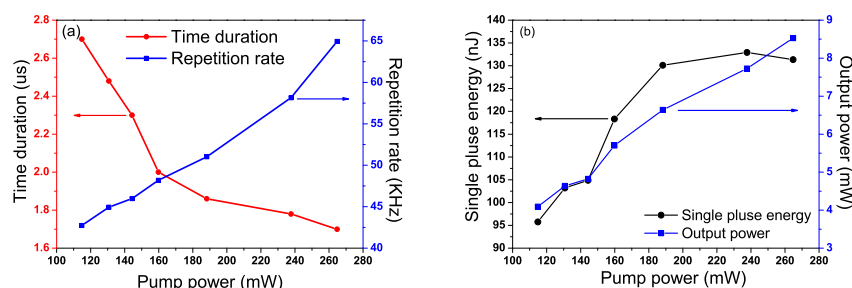


Fig. 5. (a) The pulse width and the repetition rate varies with the increasing pump power. (b) The average output power and the single pulse energy changes with the increasing pump power.

#### 4. Conclusion

We have successfully demonstrated an all-fiber passively Q-switched EDFL by using an evanescent field interaction based GNS-SA. The GNSs are optically deposited on a microfiber to ensure long nonlinear interaction length. Maximum output pulse energy of 133 nJ is obtained at repetition rate of 58.1 kHz and pulse width of 1.8  $\mu$ s from the laser cavity by the input pump power of 237 mW at 980 nm.

#### Acknowledgments

This research was supported in part by National Natural Science Foundation of China (11274224), Shanghai Shuguang Program (10SG38), and the open program (2013GZKF031307) of State Key Laboratory Advanced Optical Communication System and Networks, Shanghai Jiao Tong University. X. Zeng acknowledges the support of the Program for Professor of Special Appointment (Eastern Scholar) at Shanghai Institutions of Higher Learning.